

JPET #102376

**Tissue Distribution and Metabolism of the Tyrosine Kinase Inhibitor ZD6474 (Zactima®) in
Tumor Bearing Nude Mice Following Oral Dosing**

Daniel L. Gustafson, Erica L. Bradshaw-Pierce, Andrea L. Merz and Joseph A. Zirrolli

Department of Pharmaceutical Sciences (D.L.G., E.L.B-P., A.L.M., J.A.Z.) and The Cancer
Center (D.L.G.), University of Colorado Health Sciences Center, Denver, CO 80262

JPET #102376

Running Title: ZD6474 Pharmacokinetics in Mice

Corresponding Author: Daniel L. Gustafson, Ph.D.
School of Pharmacy, C-238
University of Colorado Health Sciences Center
4200 E. 9th Ave.
Denver, CO 80220
Tel. (303)315-0755
FAX (303)315-6281
E-mail Daniel.Gustafson@UCHSC.edu

No. Text Pages: 13

No. Tables: 4

No. Figures: 7

No. References: 28

No. Words

Abstract: 248

Introduction: 511

Discussion: 1189

Nonstandard Abbreviations: CID, collision induced dissociation; RTK, receptor tyrosine kinase; ZD6474, N-(4-Bromo-2-fluorophenyl)-6-methoxy-7-[(1-methylpiperidin-4-yl)methoxy]-quinazolin-4-amine

Recommended Section Assignment: Absorption, Distribution, Metabolism and Excretion

JPET #102376

Abstract

ZD6474 (Zactima[®]) is a tyrosine kinase inhibitor with antiangiogenic and antitumor activity currently undergoing human trials for cancer treatment. Pharmacokinetic studies in animal models are an important component in the clinical development of this agent to relate pre-clinical studies to patient treatment. In the studies presented here, the pharmacokinetics of ZD6474 was determined in plasma and tissues of MCF-7 tumor bearing nude mice following single oral doses at 10, 25, and 50 mg/kg. Plasma AUC and C_{max} were linear, increasing proportionally with dose. Tissue analysis showed that ZD6474 is extensively distributed to tissues with liver and lung accumulating concentrations of 212 $\mu\text{g/g}$ ($\sim 450 \mu\text{M}$) and 161 $\mu\text{g/g}$ ($\sim 340 \mu\text{M}$), respectively. Tumor levels ranged from 27–71 $\mu\text{g/g}$ at C_{max} levels across the three dose ranges and ZD6474 was distributed to all tissues in a dose-dependant manner. Analysis of putative ZD6474 metabolites in feces found four with the N-demethyl-piperidiny-ZD6474 metabolite being the most prominent but still accounting for less than 2% of the total amount of ZD6474 present. The lack of significant metabolism of ZD6474 is consistent with the relatively long half-life in mice (~ 30 hours) as well as that seen in humans (~ 120 hours) and the primary method of drug elimination appears to be unchanged in the feces ($\sim 25\%$). The incorporation of an empirical approach to dosing in mouse models of cancer in pre-clinical studies may allow for better prediction of clinical efficacy for ZD6474 alone and in combination with other therapeutic modalities based on equivalent drug exposure.

JPET #102376

Introduction

The processes of tumor growth and metastasis are largely regulated by signaling through receptor tyrosine kinases (RTK) in an autocrine or paracrine manner. RTK signaling processes generally involve ligand binding, dimerization and the phosphorylation of intracellular kinase domain(s) that serve as docking sites for the recruitment of other intermediates in signal transduction (Heldin, 1996). Strategies to disrupt RTK signaling pathways for cancer therapy have included anti-growth factor antibodies, receptor antagonists, anti-receptor monoclonal antibodies, anti-sense, and small molecule tyrosine kinase inhibitors (TKIs) (Levitzki et al., 1995; Ciardiello et al., 2001). The success of signal transduction inhibitors such as imatinib (Gleevec[®]) (Druker et al., 2001), gefitinib (Iressa[®]) (Herbst et al., 2002), erlotinib (Tarceva[®]) (Soulieres et al., 2004) and bevacizumab (Avastin[®]) (Hurwitz et al., 2004) in cancer therapy has had a dramatic effect on the design of clinical trials for new therapeutic regimens.

ZD6474 (N-(4-Bromo-2-fluorophenyl)-6-methoxy-7-[(1-methylpiperidin-4-yl)methoxy]-quinazolin-4-amine) belongs to a class of synthetic 4-anilinoquinazolines that are orally available and bind to the intracellular kinase domain of RTKs, preventing phosphorylation and disrupting signal transduction (Hennequin et al., 1999; Hennequin et al., 2002). ZD6474 has demonstrated potent and selective activity against the key angiogenesis vascular endothelial cell growth factor receptor (VEGFR2, Flk1/KDR) (Wedge et al., 2002), and the epidermal growth factor receptor (EGFR) (Hennequin et al., 1999). ZD6474 single agent pre-clinical models have shown tumor regression against a number of xenograft models (Wedge et al., 2002) as well as enhanced activity of cytotoxic chemotherapy (Ciardiello et al., 2003) and radiation (Damiano et al., 2005; Williams et al., 2004; Gustafson et al., 2004). ZD6474 has also been shown to act as a chemopreventive agent, blocking the formation of chemical-induced pre-neoplastic and neoplastic lesions in a rat model of mammary carcinogenesis (Heffelfinger et al., 2004).

The use of molecularly targeted agents such as ZD6474 in the clinic will probably involve combinations with other therapeutic modalities. Recent successful clinical trials combining

JPET #102376

cetuximab (Erbix[®]) with radiation therapy in squamous cell carcinoma of the head and neck (Bonner et al., 2006) as well as results with trastuzumab (Herceptin[®]) in combination with cytotoxic chemotherapy in breast cancer (Piccart-Gebhart et al., 2005) highlight therapeutic advantages gained. Considering the large numbers of potential combinations exist with various molecular targets, therapeutics, treatment schedules and a number of other factors, the importance of well planned pre-clinical studies to limit and optimize combinations that proceed to clinical trial are critical. Pre-clinical studies should be designed with dose levels and schedules that mimic both response and exposure, either predicted or previously determined, in human patient populations. This approach could potentially increase the correlation between pre-clinical and clinical successes for treatments and help negate the effect of effective dose intensities in animal models that are irrelevant to the human condition. However, this type of approach requires reliable and intensive pharmacokinetic studies in animal models. To this end, we have carried out a multiple-dose, time course pharmacokinetic study in tumor bearing nude mice for ZD6474. Drug levels were measured in plasma and tissues after oral dosing of 10, 25 and 50 mg/kg and putative metabolites analyzed in feces, liver and plasma.

JPET #102376

Methods

Cells. MCF-7 cells, purchased from ATCC (Manassas, VA), were maintained on tissue culture plates in RPMI 1640 (Cellgro, Herndon, VA) supplemented with 10% FBS (Hyclone, Logan, UT), penicillin (100 units/mL)/streptomycin (100 ug/mL) (GIBCO, Carlsbad, CA), and 0.0015 units/mL insulin (Humulin[®], Eli Lilly and Company, Indianapolis, IN). Cells were kept in a humidified atmosphere of 5% CO₂/95% air at 37°C.

MCF-7 Xenografts. Female 6-8 week old balb/c athymic nude mice were purchased from Simonsen Laboratories (Gilroy, CA). Animals were housed in polycarbonate cages and kept on 12 hour light/dark cycle. Food and water were given *ad libitum*. All studies were conducted in accordance with the National Institutes of Health guidelines for the care and use of laboratory animals, and animals were housed in facility accredited by the American Association for Accreditation of Laboratory Animal Care. Animals were allowed to acclimate for 7 days prior to any handling.

Animals were implanted with slow-release Silastic[®] 17β-estradiol pellets at least 24 hours prior to MCF-7 tumor cell inoculation. Briefly, animals were anesthetized with 75 mg/kg ketamine and 15 mg/kg xylazine (Vedco, St. Joseph, MO) via intraperitoneal injection. When animals no longer responded to toe-pinch, Silastic[®] estradiol pellets were implanted subcutaneously between the shoulders. The incision was closed with 9mm wound clips (Kent Scientific, Torrington, CT).

MCF-7 cells were harvested and resuspended in a 3:1 mixture of serum free RPMI 1640 and matrigel (BD Bioscience, Bedford, MA). Five million cells per mouse were injected subcutaneously into the rear flank using a 23 gauge needle. Tumors volumes, measured by digital calipers, were calculated by equation 1:

$$(1) \quad V(\text{mm}^3) = \text{length} \bullet \text{width} \bullet 0.5236$$

JPET #102376

Silastic® Estradiol Pellets. Silastic® estradiol pellets were prepared as described previously by Sartorius, *et al* (Sartorius et al., 2003). Silastic® tubing (1.98mm ID x 3.18mm OD, Dow Corning, Midland, MI) was cut into 1 cm pieces and autoclaved. One end of the 1 cm pieces was sealed with clear silicone rubber and allowed to dry overnight. 17 β -Estradiol (Sigma, St. Louis, MO) was added to α -cellulose (Sigma, St. Louis, MO) at a ratio of 1:4 (w/w) then mixed and ground into a fine powder with a mortar and pestle. The powder was packed into the tubing pieces with a sealed Pasteur pipette and the open end sealed with clear silicone rubber and allowed to dry overnight. Pellets contain approximately 2 mg of 17 β -estradiol.

Pharmacokinetic Studies. ZD6474 for oral administration was made as a suspension in sterile filtered 1% Tween 80 by gentle mixing with 4 mm borosilicate glass beads overnight. Mice were manually randomized into treatment groups with a weight at the beginning of study of 24.8 ± 1.9 g (median = 25.2 g) and a tumor volume of 193.2 ± 125.8 mm³ (median = 170.9 mm³) and treated with a single dose of 10, 25 or 50mg/kg ZD6474 by oral gavage. Gavage volumes varied between 90-120 μ l based on animal weight (4 μ l/g body weight). Following drug dosing, three mice per treatment group were sacrificed at 0.25, 0.5, 1, 4, 8, 24, 48, and 72 hours by cardiac stick exsanguinations under isoflurane anesthesia and plasma and tissue samples collected (liver, kidney, lung, heart, intestine, fat, muscle, brain, and tumor). Collected samples were rinsed in PBS and immediately frozen in liquid nitrogen and stored at -80°C prior to sample preparation for drug analysis. Animals to be sacrificed at 24, 48 and 72 hours post treatment were housed in metabolic cages to collect feces. Urine could not be collected due to evaporation prior to reaching the collection vesicle.

JPET #102376

For the multiple dosing pharmacokinetic analyses, four MCF-7 tumor bearing nude mice were treated with 25 mg/kg ZD6474 for seven consecutive days and animals sacrificed and tissues collected as described four hours after the last dose.

LC/MS/MS Analysis of ZD6474 and Metabolites. Analysis of ZD6474 in mouse plasma and tissues was carried out by LC/MS/MS analysis as previously described (Zirrolli et al., 2005). Briefly, 50 μ l plasma samples were mixed with 50 μ l of 10 mM ammonium acetate (pH 9.6) and 50 μ l of 1 μ g/ml trazodone (internal standard) followed by extraction with 1 ml of 1:1 ethyl acetate/pentane. For tissues, samples were homogenized using a Potter-Elvehjem Tissue Grinder with a PTFE pestle bottom in 10 mM ammonium acetate (pH 9.6) at approximately 100 mg/ml (w/v), 100 μ l aliquots were transferred to another tube containing 50 ng trazodone followed by extraction with 1 ml of 1:1 ethyl acetate/pentane. The organic layer was collected following extraction, evaporated to dryness, and re-constituted in 1 ml of acetonitrile:water (1:1, v/v). Samples were analyzed with a PE Sciex API-3000 triple quadrupole mass spectrometer (Foster City, CA) with a turbo ionspray source interfaced to a PE Sciex 200 HPLC system. The mobile phase was isocratic with 80% acetonitrile containing 10 mM ammonium acetate and 0.1% acetic acid at a flow rate of 200 μ l/min and a Discovery HS F5, 5 μ m, 120A^o, 50 x 2.1 mm column (Supelco, Bellefonte, PA) was used. Samples were quantitated by internal standard reference in multiple reaction monitoring (MRM) mode by monitoring the transition m/z 475 \rightarrow 112 for ZD6474 and the transition m/z 372 \rightarrow 176 for the internal standard (trazodone). For the extraction of feces, total collected fecal pools were mixed with water (2:1, water:feces, w/v) to make a homogenous paste that was extracted as described above.

Metabolite analysis was done on extracted samples prepared as described above. The most probable metabolism of ZD6474 would involve hydroxylation and demethylation of the methyl groups at the 6-methoxy and 1-methylpiperidinyl groups. A set of tandem mass spectrometric protocols including MRM, product ion and precursor ion scans were designed to

JPET #102376

search for these four probable metabolites. As the collision-induced dissociation (CID) fragmentation of ZD6474 is dominated by formation of the protonated N-methylpiperidinylmethylene group (m/z 112) it was assumed that neither hydroxylation nor demethylation at either methyl group would strongly affect this fragmentation mechanism. MRM scan protocols were designed to detect ZD6474 and the four possible metabolites shown in Figure 1 using calculated m/z of the precursor $[M+H]^+$ ion and the predicted CID product ions based on the formation of these putative metabolites.

Saline to Tissue Partitioning. The estimation of ZD6474 saline to tissue partitioning (K_{pT}) was done as previously described (Jepson et al., 1994) with some modification. Briefly, 1-2 mm³ tissue pieces were incubated in PBS with gently shaking at 37° C for 16 hours. Saline and tissue were separated by centrifugation at 1500g for 10 minutes, and the tissue and saline collected. The saline portion was filtered using a 10,000 dalton molecular weight cutoff filter (Centricon YM-10) by centrifugation. Tissue and saline portions were extracted and analyzed for ZD6474 as described earlier.

Pharmacokinetic and Statistical Analysis. Analysis of data for the calculation of pharmacokinetic parameters was carried out using non-compartmental analysis with WinNonlin v. 4.1 (Pharsight Corp., Mountain View, CA). Statistical analyses (Pearson correlation, linear regression) were carried out using GraphPad Prism v. 4.02 (GraphPad Software, Inc., San Diego, CA).

JPET #102376

Results

Plasma Pharmacokinetics of ZD6474. The plasma pharmacokinetic results are shown in Figure 2 and parameters as calculated using non-compartmental methods shown in Table 1. AUC and C_{\max} values were linear with dose ($r^2 > 0.99$) for each parameter. Terminal half-life ($t_{1/2\lambda}$), clearance (CL/F) and extrapolated volume of distribution (V_z/F) were consistent across doses, in line with the relationship between dose and AUC and C_{\max} in that all were features of drugs that follow linear kinetics. The time to reach C_{\max} (T_{\max}) decreased with dose (Figure 2 inset). One possible explanation for this is that ZD6474 was dosed as an oral suspension and the compound is more soluble under acidic conditions (Hennequin et al., 2002). Therefore, at higher doses a more rapid peak may have been reached due to increased dissolution and rapid absorption in the stomach prior to gastric emptying into the more pH neutral intestinal track where the dissolution rate is slower. This idea is supported by the early time course profile shown in the Figure 2 inset in that an early peak is achieved followed by a gradual decline and then a gradual increase to a second, smaller peak.

Tissue Distribution of ZD6474. The time courses of ZD6474 distribution in liver, lung, intestine, kidney, fat, brain, muscle and subcutaneous tumor xenografts were determined. The results are shown in Figure 3 and a summary of tissue pharmacokinetics in Table 2. Tissue accumulation, in accordance with plasma data, was linear with dose across all tissues with liver and lung tissue accumulating the highest concentrations. Liver drug levels at C_{\max} ranged from 40 $\mu\text{g/g}$ (~84 μM) to 212 $\mu\text{g/g}$ (~446 μM) at the 10 and 50 mg/kg doses, respectively. Analysis of saline to tissue partitioning showed that ZD6474 solubility does not vary widely amongst tissues ranging from 8.3 to 4.8 (drug in tissue:drug in saline). Taking these modest differences in partitioning in account with tissue blood flow (Brown et al., 1997), correlations with both AUC and C_{\max} in tissues were obtained. The correlation across the tissues analyzed of tissue AUC versus the product of tissue specific partitioning (K_{pT}) and tissue blood flow (Q_T) was significant

JPET #102376

($P < 0.001$) with a correlation coefficient (Pearson r value) of 0.925. The same analysis using tissue C_{\max} values was also significant ($P < 0.0013$) with a correlation coefficient (Pearson r value) of 0.918. These data strongly suggest that ZD6474 tissue uptake and distribution is perfusion limited with minimal impact of tissue diffusion.

Fecal Elimination of ZD6474. Accumulation of ZD6474 in feces was measured to determine drug elimination via this route. Fecal elimination of ZD6474 was measured for 0 to 24 hours, 24 to 48 hours and 48 to 72 hours (Table 3). Cumulative elimination over the 72 hour period was linear with dose ($r^2 = 0.996$). Interestingly, the amount of ZD6474 excreted from 48 to 72 hours was similar across dose levels. This may be due to the fecal deposition of drug that was never absorbed from the gastrointestinal (GI) tract. The time for the entire contents of the mouse GI tract to be completely eliminated has been measured at approximately 3 days (Schwarz et al., 2002), thus the accumulation of unabsorbed drug in the feces would be within this time frame.

Identification and Relative Measurement of ZD6474 Metabolites. Fecal extracts were analyzed for four putative metabolites as shown in Figure 1 and all four were detected. It was not possible to accurately quantify the extent of metabolism without valid reference standards for each metabolite but the relative MS/MS response of each metabolite to the parent drug, ZD6474, is shown in Table 4. It was clear that ZD6474 is not extensively metabolized. This conclusion assumes that the extraction, ionization and CID efficiencies of metabolites were similar to ZD6474, which is probably valid as the ionization and CID processes are directed by the very basic piperidinyl group and the addition of a hydroxyl group and/or demethylation is not likely to have a large impact on ethyl acetate:pentane solubility. Several metabolites were also detected in plasma and liver samples but at much lower levels (Table 4).

To verify that the MRM analyses were accurately detecting metabolites, product ion and precursor ion scans were performed with the feces samples. Conclusive product ion spectra

JPET #102376

were obtained for the two most abundant metabolites, N-demethyl-piperdiny-ZD6474 ($[M+H]^+$, m/z 461,463; Figure 4A) and 6-OH-methoxy-ZD6474 ($[M+H]^+$, m/z 491,493; Figure 5A). Surprisingly the products ions of the N-demethyl-piperdiny-ZD6474 included an ion pair at m/z 364, 366 indicating the loss of neutral methylene-piperidine (M 97) with charge retention on the methoxy-phenyl-4-amino-quinazoline (Figure 4A). This product ion spectrum was obtained with Q1 in low resolution and Q3 in unit resolution to demonstrate that the ion pair at m/z 364, 366 retained the bromine isotopic pattern. The product ion spectra of 6-OH-methoxy-ZD6474 was obtained with both Q1 and Q3 in unit resolution mode and clearly shows that the molecular weight of the metabolite increased by 16 amu ($[M+H]^+$, m/z 491, ^{79}Br -isotopomer) but the CID fragment ion remained at m/z 112, indicating that the site of hydroxylation was not the N-methyl piperidiny group. The remaining metabolites did not yield conclusive product ions due to their low abundance.

Further verification of the metabolites was obtained with precursor scans. Precursor scans of m/z 128 detected that this ion was a fragment ion of m/z 491,493 indicating hydroxylation on the N-methylpiperidiny group. Precursor ion scans of m/z 112 detected that this fragment ion came from two distinct ion pairs; m/z 461,463 and m/z 491,493 indicating the 6-OH-ZD6474 and 6-OH-methoxy-ZD6474 metabolites, respectively, as the methylpiperidiny group was unchanged.

Prediction and Validation of Steady State ZD6474 Plasma and Tissue Concentrations

Based on Single Dose Pharmacokinetic Data. Using the pharmacokinetic data generated from the single dose studies, predictions were made as to the steady-state levels of ZD6474 in plasma and tissues. Using a half-life value of 28 hours which is the average of the values across doses shown in Table 1, an accumulation factor was calculated with equation 2;

$$(2) \quad \text{Accumulation Factor} = \frac{1}{1 - e^{-k_{\lambda} \cdot T}}$$

JPET #102376

where k_{λ} is the elimination rate constant based on the terminal half-life ($0.693/t_{1/2\lambda}$) and T is the dosing interval (24 hours). From this equation, an accumulation factor of 2.2 was calculated for daily dosing of ZD6474 in nude mice. The accumulation factor was multiplied by the average value at 4 hours from the single dose study at 25 mg/kg and this tissue concentration is compared to that obtained following seven days consecutive dosing of ZD6474 (Figure 6). The predicted values showed good agreement with the actual measured values across tissues and validated the pharmacokinetic parameters calculated from the single dose studies for use in future dose and dosing schedule extrapolations.

JPET #102376

Discussion

The aim of this study was to define the pharmacokinetics and metabolism of ZD6474 in nude mice for use in the design of dose and schedules reflective of drug exposure achieved in humans. The pharmacokinetics of ZD6474 in humans has been studied in both Phase I dose escalation studies (Holden et al., 2005; Minami et al., 2003) as well as in Phase II trials at doses of 100 and 300 mg/day (Miller et al., 2005). The results from these studies have shown that ZD6474 is slowly absorbed (relatively small K_a), widely distributed (large volume of distribution) and slowly eliminated with an elimination half-life of approximately 120 hours (Holden et al., 2005; Minami et al., 2003). More recent PK studies in humans have suggested that the terminal half-life is longer, approaching 200 hours (Miller et al., 2005). The long elimination half-life of ZD6474 leads to accumulation with daily dosing until a steady-state level is achieved. Accumulation in Japanese patients when comparing AUC of the first dose versus AUC on day 28 of daily dosing showed a 6-14 fold accumulation with elimination half-lives varying from 72 to 167 hours (Minami et al., 2003). An approximate 7 to 10-fold accumulation has also been shown in other human studies (Holden et al., 2005).

ZD6474 tissue distribution, metabolism and fecal elimination in tumor bearing mice were addressed in the studies presented here. The results show that ZD6474 accumulated in tissues at levels up to ~100X that of plasma (liver and lung) in a manner proportional to the dose. Analysis of feces for putative metabolites identified some metabolites but they accounted for a very small proportion of the total drug in feces with the majority being parent drug. This lack of substantial *in vivo* metabolism is consistent with *in vitro* metabolism studies we have performed using mouse liver microsomal preparations that showed no significant loss of ZD6474 following two-hour incubation (data not shown). One limitation of mouse studies is the inability to quantitatively collect urine, even with the use of standard metabolic cages, due to evaporation prior to reaching the collecting vesicle. The fact that ZD6474 is highly protein bound (~95%) in the plasma, as well as highly lipophilic and thus likely to undergo substantial reabsorption along

JPET #102376

the nephron argue against substantial urinary elimination. Further, using the tissue levels that we determined and the measured fecal levels we can account for 58% of the administered dose after 24 hours while only summing 65% of the total mass of the mouse. This argues against extensive urinary elimination and suggests that that the major route of ZD6474 elimination in the mouse is fecal excretion of parent drug.

Using human pharmacokinetic data for ZD6474 from clinical trials and the data in mice determined from this study, we can calculate daily dosing in mice that will reflect human parameters in terms of drug exposure. To accomplish this, we used an accumulation factor of 7.8 calculated on a median half-life of 120 hours and applied this factor to the C_{max} , C_{min} and AUC dose-dependent values reported for single doses in humans. The calculated steady-state values were compared to those calculated in mice with the 2.2 fold accumulation factor and the human and mouse data is shown in Figure 7. Based on these calculations, to simulate daily dosing C_{max} levels that occur in humans at the 300 mg dose, mouse dosing would be 17.4 mg/kg, to simulate C_{min} levels mouse dosing would be 48.6 mg/kg, and to simulate AUC a dose of 17.8 mg/kg should be used in mice. The calculation of these doses can be easily changed to reflect the purported longer 200 hour half-life that has recently been reported (Miller et al., 2005) by calculating an accumulation factor based on the 200 versus 120 hour half-life.

Doses in mice with ZD6474 in preclinical studies have ranged from 12.5 to 150 mg/kg/day (Wedge et al., 2002; Ciardiello et al., 2003; Taguchi et al., 2004; Damiano et al., 2005). In most cases, pronounced inhibition of tumor growth or induction of tumor regression has occurred at doses above the 25 mg/kg/day level, with doses at or below this level generally leading to a slowing of tumor growth (Wedge et al., 2002). Another issue with dosing in mice is the use of *intraperitoneal* (*ip*) dosing as a substitute for the oral route. Although *ip* dosing does have similarities with oral delivery in terms of absorption of drug mostly via the intestines and the delivery of drug initially to the liver by way of the splanchnic circulation, there are differences that can have dramatic effects on pharmacokinetics. Comparison of *ip* dosing to oral gavage in

JPET #102376

terms of ZD6474 pharmacokinetics in mice has been studied in our laboratory. Dosing via the *ip* route leads to an approximate 2-fold increase in the obtained C_{\max} value (2.06 vs. 1.09 $\mu\text{g/ml}$ at 25 mg/kg dose) and 30% increase in AUC when compared to the oral route (data not shown). Presumably, this is due to a more rapid absorption of drug caused by the increased surface area presented when drug is dispensed in the peritoneal cavity as opposed to being contained within the gastrointestinal tract. This difference points out the complexity of dosing scenarios in animal models and the importance of pharmacokinetically directed guidelines.

ZD6474 is a novel, poly-targeted tyrosine kinase inhibitor that has shown activity in pre-clinical animal models and is currently undergoing Phase III evaluation for the treatment of cancer. The clinical development of ZD6474 and similar agents will involve the use of multi-drug and modality therapy with cytotoxic chemotherapy and radiation likely companions to its' use. Studies have been carried out and are ongoing in animal models on the use of ZD6474 with chemotherapy (Ciardiello et al., 2003; Morelli et al., 2005) and radiotherapy (Damiano et al., 2005; Williams et al., 2004; Gustafson et al., 2004). Carrying out animal studies with rational doses and dosing schedules of drugs comparable to use in humans is an invaluable and often ignored component of pre-clinical studies. The use of enormous doses with no relevance to the human condition is a common criticism of animal models of cancer (Leaf, 2004) and a valid one.

The clinical development of agents for the treatment of cancer is a long process with the added complexity of drug and treatment combinations along with utility in the advanced or adjuvant setting. Optimization of animal models in this process is an important component. With a drug such as ZD6474, where human pharmacokinetic data is available, comparative studies of drug disposition in animal models is a reasonable mechanism to ensure that studies are carried out using relevant doses. To this end, we have carried out pharmacokinetic studies in tumor bearing nude mice of ZD6474. The results of these studies were that ZD6474 shows linear pharmacokinetics within the relevant dose range, was minimally metabolized, and that simple multiple-dose models can be used to extrapolate both mouse and human ZD6474

JPET #102376

pharmacokinetics in order to calculate dosing scenarios that relate dosing in mice to humans. The application of this information in mouse models will allow for a more sound design and assessment of pre-clinical animal results when planning clinical trials.

Acknowledgements

The authors would like to thank Dr. Andy Ryan (AstraZeneca, Alderley Park, Macclesfield, UK) for useful discussion regarding these studies.

JPET #102376

References

Bonner JA, Harari PM, Giralt J, Azarnia N, Shin DM, Cohen RB, Jones CU, Sur R, Raben D, Jassem J, Ove R, Kies MS, Baselga J, Youssoufian H, Amellal N, Rowinsky EK and Ang KK (2006) Radiotherapy plus cetuximab for squamous-cell carcinoma of the head and neck. *N Engl J Med* 354:567-578.

Brown RP, Delp MD, Lindstedt SL, Rhomberg LR and Beliles RP (1997) Physiological parameter values for physiologically based pharmacokinetic models. *Toxicol Ind Health* 13:407-484.

Ciardiello F, Caputo R, Damiano V, Caputo R, Troiani T, Vitagliano D, Carlomagno F, Veneziani BM, Fontanini G, Bianco AR and Tortora G (2003) Antitumor effects of ZD6474, a small molecule vascular endothelial growth factor receptor tyrosine kinase inhibitor with additional activity against epidermal growth factor receptor tyrosine kinase. *Clin Cancer Res* 9:1546-1556.

Ciardiello F and Tortora G (2001) A novel approach in the treatment of cancer: targeting the epidermal growth factor receptor. *Clin Cancer Res* 7:2958-2970.

Damiano V, Melisi D, Bianco C, Raben D, Caputo R, Fontanini G, Bianco R, Ryan A, Bianco AR, De Placido S, Ciardiello F and Tortora G (2005) Cooperative antitumor effect of multitargeted kinase inhibitor ZD6474 and ionizing radiation in glioblastoma. *Clin Cancer Res* 11:5639-5644.

Druker BJ, Talpaz M, Resta DJ, Peng B, Buchdunger E, Ford JM, Lydon NB, Kantarjian H, Capdeville R, Ohno-Jones S and Sawyers CL (2001) Efficacy and safety of a specific inhibitor of the BCR-ABL tyrosine kinase in chronic myeloid leukemia. *N Engl J Med* 344:1031-1037.

JPET #102376

Gustafson DL, Merz AL, Zirrolli JA, Connaghan-Jones KD and Raben D (2004) Impact of scheduling on combined ZD6474 and radiotherapy in head and neck tumor xenografts. *Eur J Cancer* 2 (supp):54.

Heffelfinger SC, Yan M, Gear RB, Schneider J, LaDow K and Warshawsky D (2004) Inhibition of VEGFR2 prevents DMBA-induced mammary tumor formation. *Lab Invest* 84:989-998.

Heldin CH (1996) Protein tyrosine kinase receptors. *Cancer Surveys* 27:7-24.

Hennequin LF, Stokes ESE, Thomas AP, Johnstone C, Plé PA, Ogilvie DJ, Dukes M, Wedge SR, Kedrew J and Curwen JO (2002) Novel 4-anilinoquinazolines with C-7 basic side chains: design and structure activity relationship of a series of potent, orally active, VEGF receptor tyrosine kinase inhibitors. *J Med Chem* 45:1300-1312.

Hennequin LF, Thomas AP, Johnstone C, Stokes ESE, Plé PA, Lohmann J-JM, Ogilvie DJ, Dukes M, Wedge SR, Curwen JO, Kendrew J and Lambert-van der Brempt C (1999) Design and structure-activity relationships of a new class of potent VEGF receptor tyrosine kinase inhibitors. *J Med Chem* 42:5369-5389.

Herbst RS, Maddox A-M, Rothenberg ML, Small EJ, Rubin EH, Baselga J, Rojo F, Hong WK, Swaisland H, Averbuch SD, Ochs J and LoRusso PM (2002) Selective oral epidermal growth factor receptor tyrosine kinase inhibitor ZD1839 is generally well-tolerated and has activity in non-small-cell lung cancer and other solid tumors: results of a phase I trial. *J Clin Oncol* 20:3815-3825.

Holden SN, Eckhardt SG, Bassler R, de Boer R, Rischin D, Green M, Rosenthal MA, Wheeler C, Barge A and Hurwitz HI (2005) Clinical evaluation of ZD6474, an orally active inhibitor of VEGF and EGF receptor signaling, in patients with solid, malignant tumors. *Ann Oncol* 16:1391-1397.

JPET #102376

Hurwitz H, Fehrenbacher L, Novotny W, Cartwright T, Hainsworth J, Heim W, Berlin J, Baron A, Griffing S, Holmgren E, Ferrara N, Fyfe G, Rogers B, Ross R and Kabbinavar F (2004) Bevacizumab plus irinotecan, fluorouracil, and leucovorin for metastatic colorectal cancer. *N Engl J Med* 350:2335-2342.

Jepson GW, Hoover DK, Black RK, McCafferty JD, Mahle DA and Gearhart JM (1994) A partition coefficient determination method for nonvolatile chemicals in biological tissues. *Fund Appl Toxicol* 22:519-524.

Leaf C (2004) Why we're losing the war on cancer. *Fortune* March 22:77-94.

Levitzi A and Gazit A (1995) Tyrosine kinase inhibition: an approach to drug development. *Science* 267:1782-1788.

Miller KD, Trigo JM, Wheeler C, Barge A, Rowbottom J, Sledge G and Baselga J (2005) A multicenter phase II trial of ZD6474, a vascular endothelial growth factor receptor-2 and epidermal growth factor receptor tyrosine kinase inhibitor, in patients with previously treated metastatic breast cancer. *Clin Cancer Res* 11:3369-3376.

Minami H, Ebi H, Tahara M, Sasaki Y, Yamamoto N, Yamada Y, Tamura T and Saijo N (2003) A phase I study of an oral VEGF receptor tyrosine kinase inhibitor ZD6474, in Japanese patients with solid tumors. *Proc Amer Assoc Clin Oncol* 22:194.

Morelli MP, Cascone T, Troiani T, De Vita F, Orditura M, Laus G, Eckhardt SG, Pepe S, Tortora G and Ciardiello F (2005) Sequence-dependent antiproliferative effects of cytotoxic drugs and epidermal growth factor receptor inhibitors. *Ann Oncol* 16:iv61-iv68.

Piccart-Gebhart MJ, Procter M, Leyland-Jones B, Goldhirsch A, Untch M, Smith I, Gianni L, Baselga J, Bell R, Jackisch C, Cameron D, Dowsett M, Barrios CH, Steger G, Huang CS,

JPET #102376

Andersson M, Inbar M, Lichinitser M, Lang I, Nitz U, Iwata H, Thomssen C, Lohrisch C, Suter TM, Ruschoff J, Suto T, Greatorex V, Ward C, Straehle C, McFadden E, Dolci MS, Gelber RD and the Herceptin Adjuvant (HERA) Trial Study Team (2005) Trastuzumab after adjuvant chemotherapy in HER2-positive breast cancer. *N Engl J Med* 353:1659-1672.

Sartorius CA, Shen T and Horowitz KB (2003) Progesterone receptors A and B differentially affect the growth of estrogen-dependent human breast tumor xenografts. *Breast Cancer Res* 79:287-299.

Schwarz R, Kaspar A, Seelig J and Künnecke B (2002) Gastrointestinal transit times in mice and humans measured with ^{27}Al and ^{19}F nuclear magnetic resonance. *Magn Reson Med* 48:255-261.

Soulieres D, Senzer NN, Vokes EE, Hidalgo M, Agarwala SS and Siu LL (2004) Multicenter phase II study of erlotinib, an oral epidermal growth factor receptor tyrosine kinase inhibitor, in patients with recurrent or metastatic squamous cell cancer of the head and neck. *J Clin Oncol* 22:77-85.

Taguchi F, Koh Y, Koizumi F, Tamura T, Saijo N and Nishio K (2004) Anticancer effects of ZD6474, a VEGF receptor tyrosine kinase inhibitor, in gefitinib ("Iressa")-sensitive and resistant xenograft models. *Cancer Sci* 95:984-989.

Wedge SR, Ogilvie DJ, Dukes M, Kendrew J, Chester R, Jackson JA, Boffey SJ, Valentine PJ, Curwen JO, Musgrove HL, Graham GA, Hughes GD, Thomas AP, Stokes ESE, Curry B, Richmond GHP, Wadsworth PF, Bigley AL and Hennequin LF (2002) ZD6474 inhibits endothelial growth factor signaling, angiogenesis, and tumor growth following oral administration. *Cancer Res* 62:4645-4655.

Williams KJ, Telfer BA, Brave S, Kendrew J, Whittaker L, Stratford IJ and Wedge SR (2004)

JPET #102376

ZD6474, a potent inhibitor of vascular endothelial growth factor signaling, combined with radiotherapy: schedule-dependent enhancement of antitumor activity. *Clin Cancer Res* 10:8587-8593.

Zirrolli JA, Bradshaw EL, Long ME and Gustafson DL (2005) Rapid and sensitive LC/MS/MS analysis of the novel tyrosine kinase inhibitor ZD6474 in mouse plasma and tissues. *J Pharm Biomed Anal* 39:705-711.

JPET #102376

Footnotes

This work was supported by CA101988 from the National Cancer Institute to DL Gustafson.

JPET #102376

Legends for Figures

Fig. 1. Structure of ZD6474, putative metabolites and predicted CID transitions.

Fig. 2. Plasma concentration versus time of ZD6474 in nude mice with MCF-7 xenografts following oral dosing. Values represent the mean \pm S.D. of three animals at each time point for each dose. Inset shows 0 to 4 hour time points.

Fig. 3. Tissue concentration versus time of ZD6474 in the (A) liver, (B) lung, (C) intestine, (D) kidney, (E) tumor, (F) fat, (G) brain and (H) muscle of nude mice with MCF-7 xenografts following oral dosing at 10 (squares), 25 (circles) and 50 (down triangles) mg/kg.

Fig. 4. (A) Product ion spectrum of m/z 461/463 showing the formation of m/z 98 ion. (B) Proposed origin of the m/z 98 product ion from the m/z 461/463 precursor for putative N-demethyl-piperidiny-ZD6474 metabolite via collision induced dissociation.

Fig. 5. (A) Product ion spectrum of m/z 491 showing the formation of m/z 112 ion. (B) Proposed origin of the m/z 112 product ion from the m/z 491 precursor for putative 6-OH-methoxy-ZD6474 metabolite via collision induced dissociation.

Fig. 6. Comparison of predicted (filled) versus measured (open) ZD6474 concentrations in (A) plasma and (B) tissues under steady-state multiple dosing conditions 4 hours after the last dose at 25 mg/kg. Predicted values were calculated from single dose data and the accumulation factor calculated as described in the text. Values represent the mean \pm S.D. of measurements made in three animals.

JPET #102376

Fig. 7. Relationship of dose to steady-state plasma (A) AUC, (B) maximal concentration (C_{\max}) and (C) minimum concentration (C_{\min}) in mice (up triangles) and humans (circles) for ZD6474. Mouse daily dosing is expressed in mg/kg and human dosing in mg/day. Values at each dose were calculated from single-dose values using the species specific accumulation factors as described in the text. Human values are from Holden *et al.* (2005). *Annals of Oncology* 16:1391.

JPET #102376

Table 1. Plasma pharmacokinetics of ZD6474 following oral dosing in mice at 10, 25 and 50 mg/kg

Data representing the average of three animals at each time point per dose were used for the construction of plasma concentration versus time curves (Figure 2). Non-compartmental modeling was used for the calculation of pharmacokinetic parameters based on the composite data.

| Dose (mg/kg) | AUC_{0→72h} ((μg/ml)•hr) | C_{max} (μg/ml) | t_{1/2}λ (hr) | T_{max} (hr) | CL/F (L/hr/kg) | V_z/F (L/kg) |
|-------------------------------|--|---|---|---------------------------------------|---------------------------------|---|
| 10 | 16.03 | 0.590 | 27.8 | 1 | 0.525 | 21.1 |
| 25 | 30.35 | 1.087 | 31.6 | 0.5 | 0.637 | 29.1 |
| 50 | 59.13 | 2.058 | 24.7 | 0.25 | 0.705 | 26.0 |

JPET #102376

Table 2. Tissue pharmacokinetics following oral dosing of ZD6474

Data representing the average of three animals at each time point per dose per tissue were used for the construction of concentration versus time curves (Figure 3). AUC was calculated by the trapezoid method and tissue disappearance half-life ($t_{1/2}$) calculated from the terminal, linear portion of the curves.

| Tissue | Dose (mg/kg) | AUC_{0→72} ((μ g/g)•hr) | C_{max} (μ g/g) | C_{min} (μ g/g) | t_{1/2} (hr) |
|---------------|---------------------|---|---|---|-----------------------------|
| Brain | 10 | 139 | 4.31 | 0.64 | 25.2 |
| | 25 | 227 | 7.68 | 1.06 | 31.9 |
| | 50 | 527 | 21.51 | 2.63 | 21.0 |
| Fat | 10 | 554 | 13.78 | 2.54 | 33.7 |
| | 25 | 1093 | 26.89 | 6.99 | 40.3 |
| | 50 | 2380 | 48.29 | 24.32 | 71.0 |
| Heart | 10 | 195 | 5.52 | 0.73 | 26.9 |
| | 25 | 458 | 10.61 | 2.20 | 32.5 |
| | 50 | 815 | 21.20 | 6.81 | 57.9 |
| Intestine | 10 | 1258 | 45.96 | 4.68 | 24.5 |
| | 25 | 3453 | 66.14 | 10.45 | 18.0 |
| | 50 | 4588 | 156.48 | 23.62 | 37.5 |
| Kidney | 10 | 1117 | 30.72 | 3.06 | 20.2 |
| | 25 | 2472 | 49.03 | 10.27 | 23.2 |
| | 50 | 5278 | 138.36 | 38.28 | 46.5 |
| Liver | 10 | 1207 | 39.54 | 2.38 | 18.3 |
| | 25 | 3321 | 82.48 | 14.85 | 22.6 |
| | 50 | 6742 | 212.25 | 59.74 | 35.4 |
| Lung | 10 | 1534 | 38.62 | 7.17 | 29.8 |
| | 25 | 3599 | 74.07 | 17.95 | 32.8 |
| | 50 | 7335 | 161.33 | 49.41 | 32.5 |
| Muscle | 10 | 207 | 4.54 | 0.15 | 17.0 |
| | 25 | 533 | 10.59 | 2.12 | 20.7 |
| | 50 | 1115 | 21.56 | 9.35 | 66.5 |
| Tumor | 10 | 765 | 26.72 | 4.49 | 30.6 |
| | 25 | 1591 | 32.62 | 14.61 | 41.4 |
| | 50 | 3573 | 71.35 | 39.06 | 70.5 |

JPET #102376

Table 3. Fecal elimination of ZD6474 following oral dosing in tumor bearing nude mice at 10, 25, and 50 mg/kg

Mice were grouped per dose level in metabolic cages and feces collected in 24-hour periods. Nine animals were included in the 0 → 24 hour group, six animals in the 24 → 48 hour group, and three animals in the 48 → 72 hour group.

| Dose (mg/kg) | Time (hr) | Total ZD6474 (µg) | % Dose | µg ZD6474 in feces/mouse |
|--------------|-----------|-------------------|--------|--------------------------|
| 10 | 0 → 24 | 411 ± 49 | 18.4 | 45.7 ± 7.0 |
| | 24 → 48 | 43 ± 22 | 2.9 | 7.1 ± 3.7 |
| | 48 → 72 | 81 ± 6 | 10.9 | 27.1 ± 2.0 |
| 25 | 0 → 24 | 666 ± 87 | 11.9 | 74.0 ± 9.7 |
| | 24 → 48 | 88 ± 11 | 2.4 | 14.7 ± 1.8 |
| | 48 → 72 | 147 ± 56 | 7.9 | 49.0 ± 18.7 |
| 50 | 0 → 24 | 1365 ± 86 | 12.2 | 151.7 ± 9.6 |
| | 24 → 48 | 285 ± 67 | 3.8 | 47.5 ± 11.2 |
| | 48 → 72 | 122 ± 23 | 3.3 | 40.6 ± 7.7 |

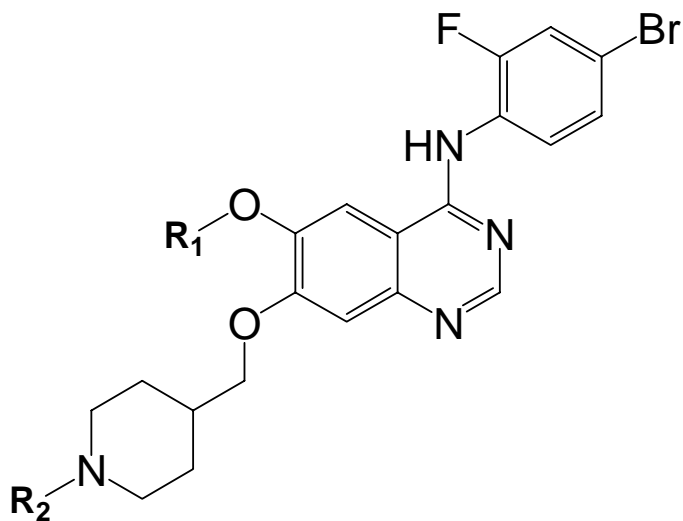
JPET #102376

Table 4. Relative abundance of ZD6474 metabolites in feces, liver and plasma of tumor bearing nude mice treated at 50 mg/kg.

Pooled fecal samples and representative liver and plasma samples were analyzed by LC/MS/MS for ZD6474 metabolites. The values represent the relative abundance of metabolites compared to parent ZD6474 in the sample. Metabolites are defined as; I, N-demethyl-piperidinyl-ZD6474; II, 6-OH-ZD6474; III, 6-OH-methoxy-ZD6474; and IV, N-OH-methyl-piperidinyl-ZD6474. ND denotes that the metabolite was undetectable in the sample.

| | Metabolite Relative Abundance (% of ZD6474) | | | |
|-----------------|--|-----------|------------|-----------|
| | I | II | III | IV |
| Feces (0→24 hr) | 1.79 | 0.04 | 0.56 | 0.16 |
| Liver (4 hr) | 0.34 | ND | ND | ND |
| Liver (8 hr) | 0.47 | ND | 0.11 | ND |
| Plasma (4 hr) | 0.43 | ND | ND | ND |
| Plasma (8 hr) | 0.71 | ND | ND | ND |

Figure 1



| Compound Name | R1 | R2 | <i>m/z</i> | |
|-----------------------------------|--------------------|--------------------|--------------------|---------|
| | | | [M+H] ⁺ | CID Ion |
| ZD6474 | CH ₃ | CH ₃ | 475 | 112 |
| 6-OH-methoxy-ZD6474 | HO-CH ₂ | CH ₃ | 491 | 112 |
| 6-OH-ZD6474 | H | CH ₃ | 461 | 112 |
| N-hydroxy-methyl-piperdiny-ZD6474 | CH ₃ | HO-CH ₂ | 491 | 128 |
| N-demethyl-piperdiny-ZD6474 | CH ₃ | H | 461 | 98 |

Figure 2

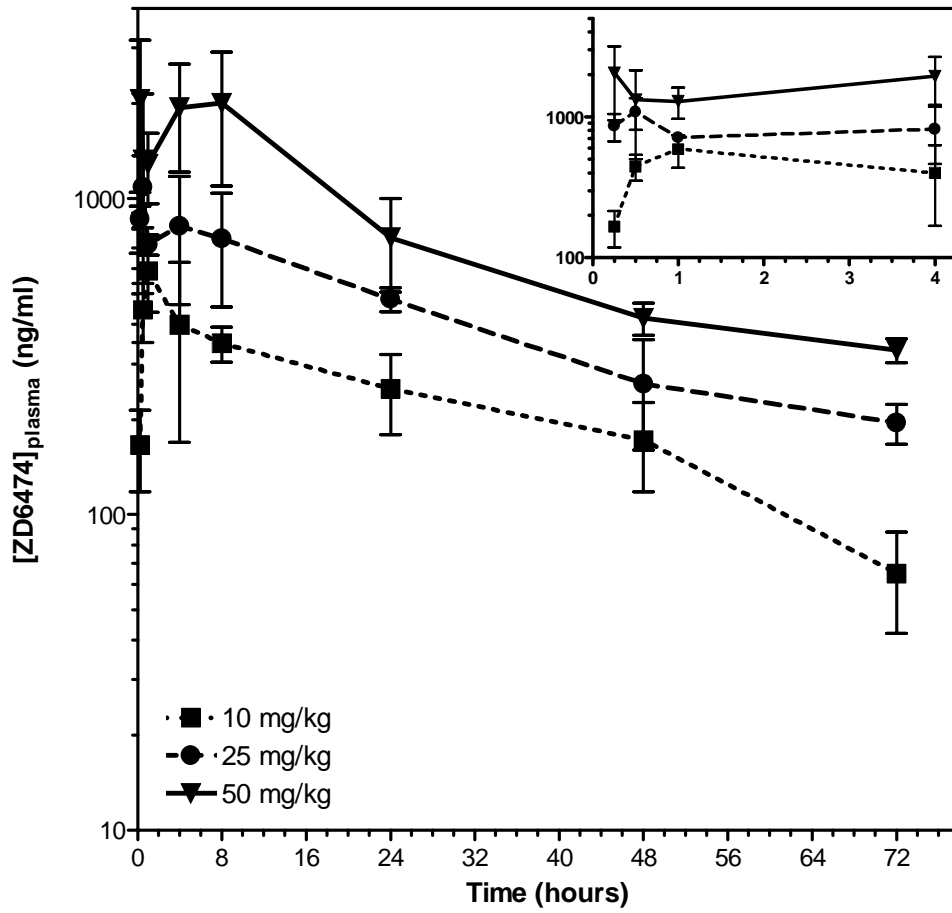


Figure 3

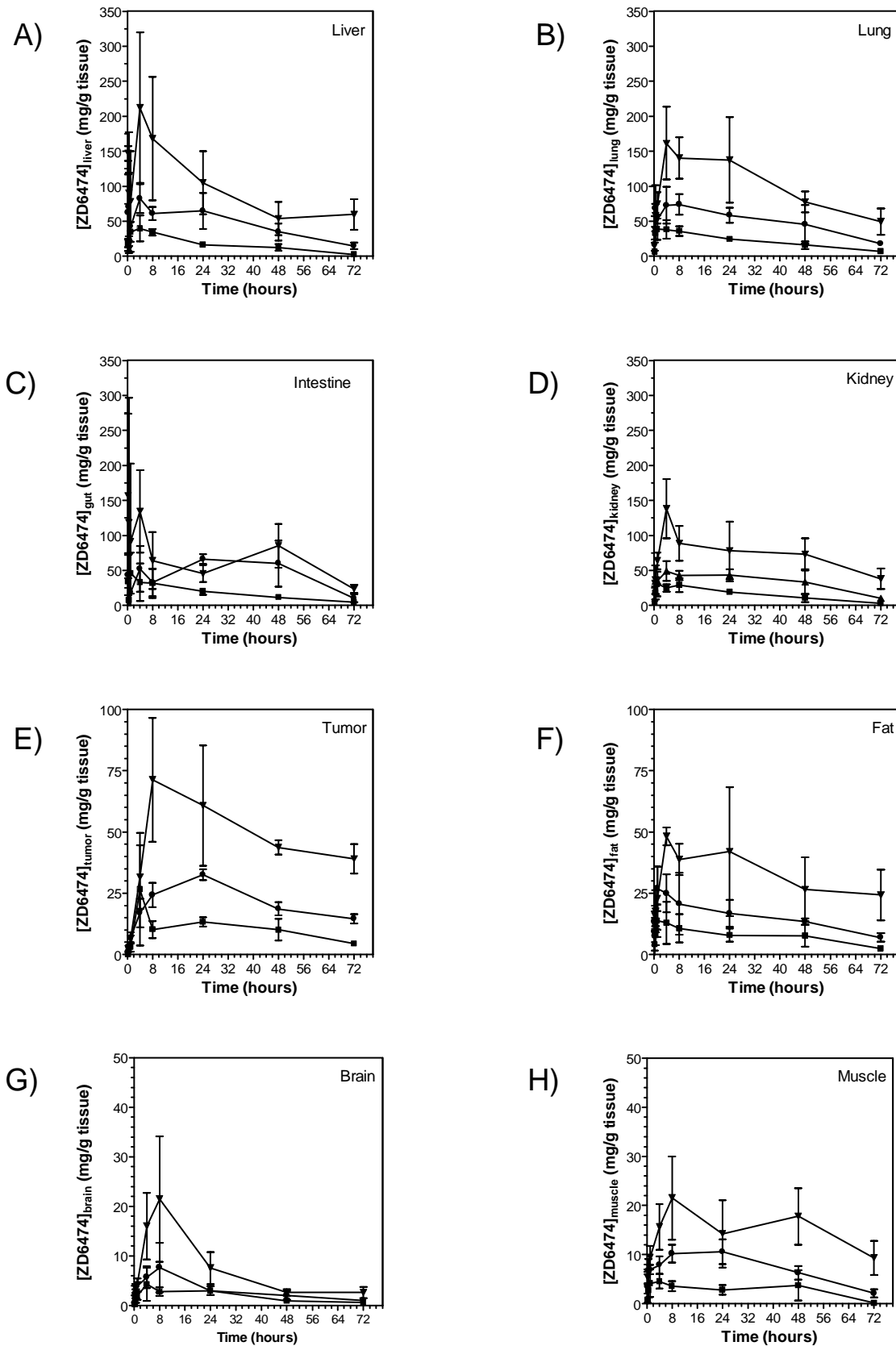
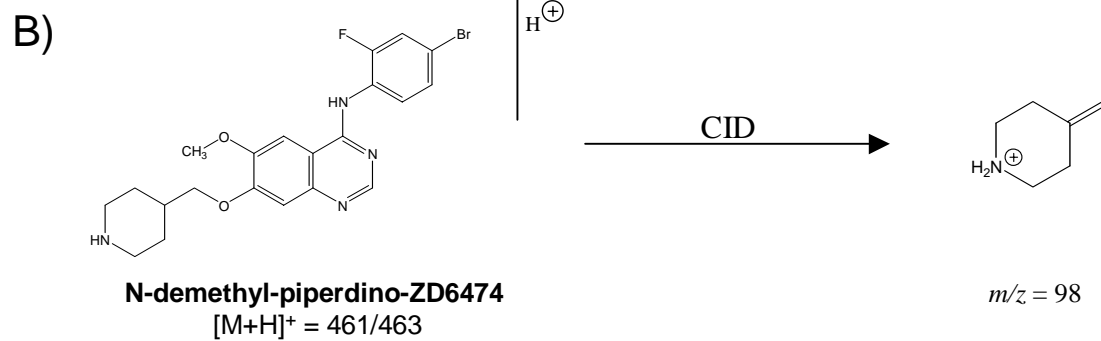
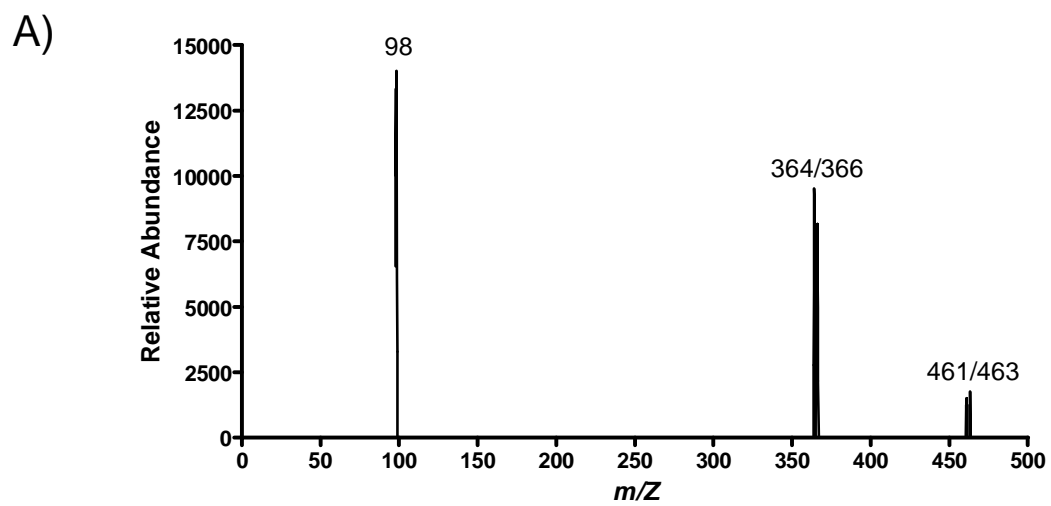


Figure 4



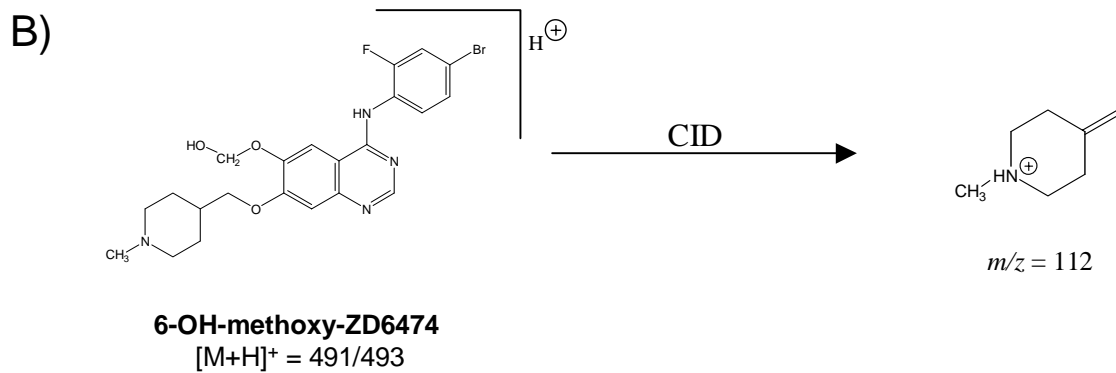
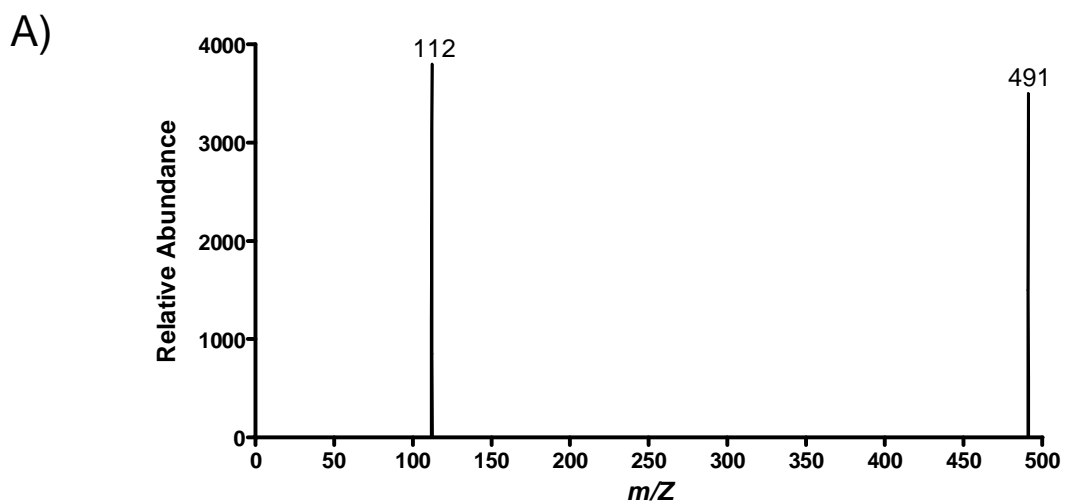


Figure 6

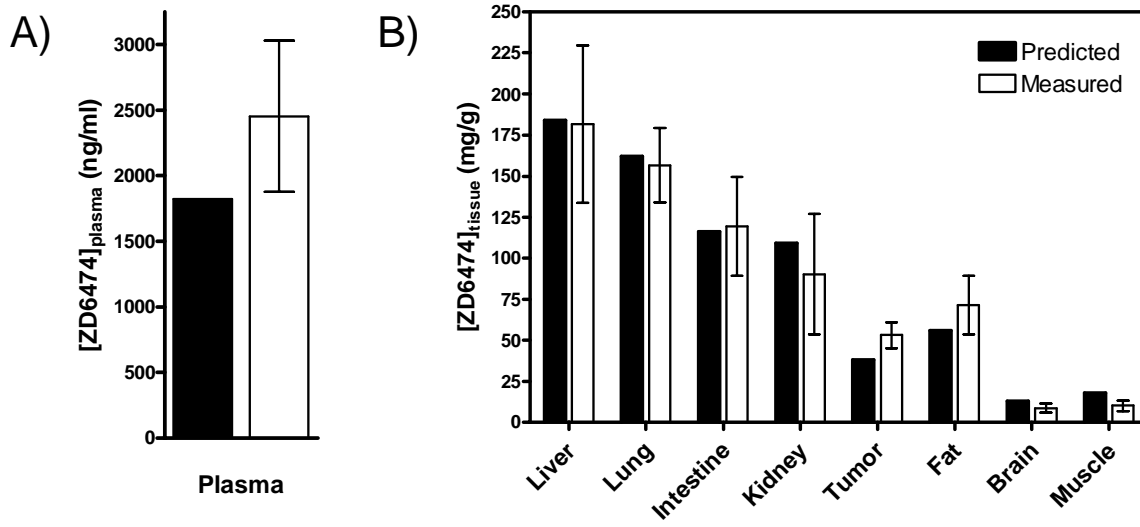


Figure 7

